Supporting Information

Li et al. 10.1073/pnas.1302770110

SI Materials and Methods

Noise exposure. ICR (CD-1) mice [postnatal day (P)17–P20], both male and female, were used for this study. Animals were handled according to methods approved by the Institutional Animal Care and Use Committee of the University of Pittsburgh. For the noise-exposed group, mice were anesthetized with isoflurane and were given unilateral noise exposure into the left ear. Narrow bandpass noise with a 1-kHz bandwidth centered at 16 kHz was presented at 116 dB sound pressure level (SPL) for 45 min. For sham-exposed (control) mice, the procedures were identical with the induced mice but no noise was presented (sham exposure).

Behavior. Gap detection, prepulse inhibition (PPI), and auditory brainstem response (ABR) threshold were tested before and 1 wk (6–7 d) after sham- or noise exposure. Gap detection paradigm (1, 2) was performed using narrow bandpass sound with a 1-kHz bandwidth centered at 10, 12, 16, 20, 24, and 32 kHz presented at 70 dB SPL. A 50-ms sound gap was introduced 130 ms before the startle stimulus. Startle response represents the time course of the downward force (presented as arbitrary units, AU) that the mouse applies onto the platform in response to the startle stimulus. Gap detection was evaluated by the gap startle ratio, which is the ratio of the peak-to-peak value of the startle waveform in trials with gap over the peak-to-peak amplitude of the startle waveform in trials in the absence of the gap. Noise-exposed mice that showed an increase in gap startle ratio by more than 0.3 in at least one tested frequency were considered as tinnitus mice (Fig. S1; detailed criteria in *Criteria for the Behavioral Evidence of Tinnitus*, below). PPI is the inverse of gap detection. PPI was tested in a quiet background, and a 50-ms nonstartling sound (prepulse)—of similar intensity to the background sound used in the gap detection test—was presented 130 ms before the startle stimulus. Prepulse inhibition was evaluated by PPI startle ratio, which is the ratio of the peak-to-peak value of the startle waveform in trials with prepulse over the peak-to-peak value of the startle waveform in startle only trial. The hearing thresholds of left ear of sham- and noise-exposed mice were measured using ABR measurements. Measurements were conducted in a sound-attenuating chamber with subdermal electrodes placed at the vertex, ground electrode placed ventral to the right pinna, and the reference electrode ventral to the left pinna. Mice were anesthetized with isoflurane with temperature maintained around 36.5–38.5 °C by a heating pad. ABR thresholds were obtained for clicks as well as tone bursts of 10, 12, 16, 20, 24, and 32 kHz.

Criteria for the Behavioral Evidence of Tinnitus. To ensure that the mouse is able to detect the gap in the background sound before noise- or sham exposure, gap startle ratio for a single test frequency before exposure is required to be below 0.9. To control for potential prepulse excitation effects, the gap startle ratio after exposure is required to be below 1.1. Frequencies that meet the above requirements are considered as valid frequencies and were used for further analysis. To determine whether a valid frequency is a tinnitus or a nontinnitus frequency, we measured and analyzed the variability of changes in gap detection in sham-exposed (control) mice before and 1 wk after sham exposure. The probability distribution of changes in gap startle ratio in control group was fitted with a normal distribution (Fig. S1; mean $\mu = -0.01$, SD $\delta = 0.15$). Because 2δ point on the upper tail marked a gap ratio increase of 0.3, the probability that the gap ratio increases more than 0.3 in a sham-exposed mouse is less than 2.2%. On the basis of this analysis, we identified a valid frequency as tinnitus frequency only if the increase in gap ratio for this frequency was more than 0.3; otherwise this frequency was a nontinnitus frequency. After assesing all six background frequencies in each mouse, we considered the mouse as a tinnitus mouse if it showed at least one tinnitus frequency. Mice that had valid frequencies but did not have any tinnitus frequency were considered as nontinnitus mice. Mice that did not have any valid frequency were not included for further analysis/experiments [uncertain group, 7 of 42 (16.7%); Fig. S1]. Taking into consideration the number of valid frequencies for each control mouse (2–6), the probability of detecting a control mouse as tinnitus mouse [i.e., the false-positive (or spontaneous, not noise-induced, tinnitus] rate is 9.2%, which is calculated by

$$P = \sum_{i=2}^{6} p_i \times \left(1 - 0.978^i\right),$$

where p_i is the probability of having i valid frequency points in a tested mouse. This value matched our experimental findings, in which 2 of 18 (11.1%) control mice were considered as having tinnitus.

Behavioral Testing with Retigabine. ICR (CD-1) mice (P17–P20), both male and female, were randomly assigned into two groups (16 mice for each group): noise-exposed treated with retigabine (retigabine group) and noise-exposed treated with vehicle (0.9% saline, saline group). All mice were first assessed for gap detection, PPI, and ABR threshold before noise exposure. For the retigabine group, retigabine (as its dihydrochloride salt; Santa Cruz Biotechnology, LKT Laboratories) was dissolved in 0.9% saline and administered 30 min after noise exposure via i.p. injection at a dose of 10 mg/kg. In the saline group the same dose of 0.9% saline was administered via i.p. injection. Both retigabine and saline were further administered twice per day for 5 d every 12 h. Gap detection, PPI, and ABR threshold were retested 24–48 h after the final injection, at which time retigabine was out of the body system (3).

Slice Preparation. Coronal slices (210 μm) of the left dorsal cochlear nucleus (DCN) were prepared from sham- and noise-exposed mice 1 wk after exposure (P24–P27). Whole-cell current clamp, voltage clamp, and loose cell-attached recordings were obtained from visually identified fusiform cells confirmed by morphological and electrophysiological characteristics (4). The incubation and external recording solution contained (in mM): 130 NaCl, 3 KCl, 1.2 KH_2PO_4, 2.4 $CaCl_2.2H_2O$, 1.3 $MgSO_4$, 20 $NaHCO_3$, 3 NaHEPES, and 10 D-glucose, saturated with 95% O_2/5% CO_2. All experiments were conducted with excitatory and inhibitory synaptic transmissions blocked by 2,3-dihydroxy-6-nitro- 7-sulfamoylbenzo[f] quinoxaline (NBQX) (10 μM) or 6,7-dinitroquinoxaline-2,3-dione(DNQX) (20 μM), SR95531 (20 μM), and strychnine (0.5 μM). Recordings were performed with temperature controlled between 34 °C and 37 °C by an inline heating system with perfusion speed maintained (4–6 mL/min).

Electrophysiological Recordings. For whole-cell voltage- and current clamp experiments, pipettes (3–5 MΩ) were filled with a K-based internal solution containing (in mM): 113 K-gluconate, 4.5 $MgCl_2.6H_20$, 14 Tris·phosphocreatine, 9 Hepes, 0.1 EGTA, 4 Na_2ATP, 0.3 Tris·GTP, 10 sucrose (pH 7.3), and 300 mOsmol. Liquid junction potential of −11 mV was corrected. Access resistance was monitored throughout the experiment from

the size and shape of the capacitive transient in response to a 5-mV depolarization step. Recordings with access resistance larger than 15 MΩ were eliminated. For whole-cell voltage clamp experiments, fast, slow capacitive currents as well as series resistance (Rs) were compensated (60–80%, bandwidth 15 kHz). In voltage clamp ramp experiments, external $CsCl_2$ (1 mM) and $CdCl_2$ (200 μM) were used to block hyperpolarization-activated cyclic nucleotide-gated channels (HCN, Ih channel) and calcium channels, respectively. For loose cell-attached voltage-clamp recording, pipettes (1.5–2.5 MΩ) were filled with modified external solution containing (in mM): 125 NaCl, 2.5 KCl, 1.25 NaH_2PO4, 2 $CaCl_2.2H_2O$, 1 $MgCl_2$, 25 $NaHCO_3$, and 25 glucose. Seal resistance was maintained between 10 and 20 MΩ with command potential at 0 mV. Recordings were performed with Clampex 10.2 and Multiclamp 700B amplifier interfaced with a Digidata 1440A data acquisition system (Axon Instruments).

Data Analysis. All protocols, except for the gap-free recording in current clamp, were applied below 0.1 Hz to eliminate potential short-term plasticity effects. In voltage-clamp step protocol for measuring KCNQ currents (Figs. 2*A* and 3*E*), tail-current amplitude was measured as the difference between the initial peak amplitude and averaged response for the last 200 ms. Step and ramp protocols (whole-cell recording) for studying KCNQ currents were applied after obtaining 5 min of stable KCNQ currents amplitude before drug application and 5 min of stable amplitude after drug application (Figs. 2*A* and 3 *E–I*). Because spontaneous firing rate of fusiform cells is not affected by the recording mode (5), we combined whole-cell and cell-attached recordings to measure spontaneous firing rates in Fig. 1 *H* and *I*. For current clamp ramp protocols, hyperpolarization current was first applied to maintain stable membrane potential at −76 mV (Fig. 3 *C* and *D*). Threshold current ($I_{threshold}$) was measured as the ramp current at which peak of the first spike was detected (Fig. 3*D*). For cell-attached recordings of the time course of the effect of XE991 on the spontaneous firing of fusiform cell (Fig. 2 *D–F*), data were normalized to the mean firing rate of the 5 min before drug application. Firing frequency was measured every 1 min by averaging the firing rate of 10 consecutive spikes. Resting membrane potential was measured with whole-cell current clamp (0 pA holding current) 5 min after TTX (0.5 μM) application when a stable membrane potential was obtained. XE991 was applied on top of TTX for its effect on resting membrane potential (Fig. 3*A*). Spike parameters were analyzed from spontaneous firing spikes with holding current I = 0 pA (synaptic transmission was pharmacologically blocked). For each fusiform cell, 20 consecutive spikes with SD of instantaneous firing rate smaller than 2 Hz were aligned at the peak and averaged. Spike threshold was measured in phase plane as the membrane potential at which the depolarization slope shows the first abrupt change (Δslope > 10 V/s; Fig. 3*B*). Input resistance was measured with small current steps at subthreshold potentials. Spike amplitude is the voltage difference between spike threshold and peak amplitude of the spike. Depolarization and hyperpolarization slope indicate the maximum slope during the depolarization and the minimum slope during hyperpolarization phase of the spike. Half height width is the width of the spike when voltage equals to (spike threshold + spike amplitude/2). Fast afterhyperpolarization (fAHP) is the voltage difference between spike threshold and spike undershoot. For Fig. 3*C*, rate of depolarization = [spike threshold (mV) − (−60 mV)]/[time from −60 mV to spike threshold]. In voltage-clamp ramp experiments, XE991-sensitive KCNQ currents elicited by slow voltage ramp (10 mV/s) were converted to conductance (G, nS) according to Ohm's law: $G = I/(V - V_r)$. I (pA) is the current amplitude at the membrane potential V (mV), and V_r is the reversal potential of potassium [−85.5 mV (5)]. Conductance–voltage curves were then fitted with Boltzmann function to describe the voltage dependence of KCNQ activation (Fig. 3 *H* and *I*):

$$G = \frac{G_{max}}{1 + e^{-(V - V_{half})/k}},$$

where G_{max} (nS) is the maximal conductance, V_{half} (mV) is the voltage for half-maximal activation, and k is the slope factor (mV). To assess the concentration dependence tetraethylammonium chloride (TEA) blockade, percentage of blocking (Y) with different concentration of TEA (x) was fitted with the Hill equation (Fig. 3*E*):

$$Y = \frac{B_{max} x^h}{IC_{50}^h + x^h}.$$

B_{max} is the maximum percentage of blocking, IC_{50} is the half-maximum blocking concentration, and h is the Hill coefficient. Analysis was performed on Igor Pro Software 5.05A, GraphPad Prism 5, and MATLAB 2011a.

Statistics. Statistical significance for behavior data were evaluated with a two-tailed paired or unpaired Student's t test (normality confirmed by Lilliefors test). The Mann-Whitney test was applied for behavioral data that did not pass the normality test. For electrophysiological data, we assumed that the population distribution follows normal distribution and evaluated with a two-tailed Student's t test or a one-way ANOVA (Tukey's honestly significant difference test for the post hoc test). We applied a binomial test for comparing ratio of tinnitus mice among different groups. Summary data are reported as means ± SEM.

More-Detailed Materials and Methods. ***Noise exposure.*** Mice were anesthetized with 3% isoflurane in oxygen; after stabilization, the anesthesia level was maintained at 1–1.5%. A pipette tip was fixed onto the speaker (CF-1; Tucker Davis Technologies) and was inserted into the left ear canal of the mouse (unilateral noise exposure).

Gap detection. Mice were confined in custom-made housing constructed of Lego parts and a small plastic container with cardboard plate and placed on a load-cell platform (E45-11; Coulbourn Instruments) inside a sound-attenuating chamber (ENV-022SD; Med Associates). The ambient sound in the chamber was 46 dB SPL (4–40 kHz). All sounds were presented through a planar isodynamic tweeter (RT2H-A; HiVi), which was positioned in front of the animal to reduce standing wave resonances. Testing was done using narrow bandpass sound with a 1-kHz bandwidth centered at 10, 12, 16, 20, 24, and 32 kHz presented at 70 dB SPL. For each trial this background sound was presented randomly for 8–25 s. Testing sessions began with 20 startle-only trails (white noise burst at 104 dB SPL for 20 ms) to habituate the evoked startle response. Startle-only trials and gap trials were presented in an alternating fashion (the gap detection trial was always before the startle-only trial). Startle-only trials were identical to gap detection trials except that a 50-ms silent gap was introduced; the startle stimulus was presented 80 ms after the cessation of the silent gap. Background frequency was presented for three times in an ascending fashion in repeat of four trials, thus allowing each frequency to be presented 12 times. For each frequency, 12 gap startle ratios were collected and averaged. Baseline movement (not induced by startle) was analyzed for the engagement level of a mouse to the startle-dependent test. Only mice that showed the baseline under 0.1 AU were used.

Prepulse inhibition. In PPI trials, a 50-ms, 70-dB SPL bandpass sound with 1-kHz bandwidth centered at 10, 12, 16, 20, 24, and 32 kHz was presented 130 ms before a startle stimulus (20 ms at 104 dB SPL). Testing sessions began with 20 startle-only trials.

PPI trials and startle-only trials were presented in an alternating fashion (the PPI trial was always presented before the startle-only trial). Frequencies were presented in an ascending fashion, with each frequency being presented five times.

Auditory brainstem responses. ABR thresholds were measured immediately after gap detection and PPI test. Measurements were conducted in a sound-attenuating chamber (ENV-022SD; Med Associates). Mice were anesthetized initially with 3% isoflurane in oxygen, which was then maintained at 1–1.5%. To present the sound stimuli, a pipette tip was fixed to the end of a plastic tube (2.5 cm in length), which was attached to the speaker (CF-1; Tucker Davis Technologies) and was inserted into the left ear canal. ABR thresholds were obtained for 1-ms clicks and 3-ms tone bursts of 10, 12, 16, 20, 24, and 32 kHz presented at a rate of 18.56/s. Stimuli were produced using the System 3 software package from Tucker Davis Technologies. Evoked potentials were averaged 1,024 times and filtered using a 300- to 3,000-Hz bandpass filter.

Behavioral experiments with retigabine. After the initial injection of retigabine the mice showed slight motor impairment, tremor, and increase in appetite. These symptoms were diminished 2–3 h later; by the third day all of these behavior symptoms were not apparent after injection of retigabine.

Slice preparation. Fusiform cells were visualized using an Olympus upright microscope (BX51w1, 40× optics) under oblique illumination condenser equipped with a XC-ST30 CCD camera and analog monitor.

Electrophysiological recordings. KH_2PO_4-free external solution was used for studying the voltage-dependent property of KCNQ currents, to prevent precipitation with bath-applied $CdCl_2$ (200 μM, see below). NBQX (10 μM; Abcam) or DNQX (20 μM; Abcam), strychnine (0.5 μM; Sigma-Aldrich), SR95531 (20 μM; Abcam) were used to block glutamatergic, glycinergic, and GABAergic synaptic transmission. XE991 (10 μM; Abcam) was applied for blocking KCNQ currents. TTX (0.5 μM; Abcam) was used to block spiking activity. TEA (Abcam) and UCL2077 (3 μM; Sigma-Aldrich) were used for assessing the subunit composition of KCNQ currents. All of the drugs were dissolved in deionized water, except for UCL2077, which used DMSO as vehicle; the final DMSO concentration was less than 0.5%. Drugs were prepared as stock solution, diluted to the final concentration immediately before using, and applied through bath perfusion. Recordings were performed with temperature controlled between 34 °C and 37 °C by an inline heating system (Warner Instruments) with perfusion speed maintained (4–6 mL min^{-1}). To monitor Rs throughout the experiment, we did not perform Rs compensation in the experiments included in Fig. 2*A* (more than 20% in Rs during the experiment led to the exclusion of the experiment; initial Rs was 8–12 MΩ for all these recordings). Whole-cell recordings were routinely terminated within 30 min after breaking in. For cell-attached recordings, slight adjustment (−5 mV to 5 mV) was given to ensure that the amplifier read 0 pA at the baseline potential. Spike peak-to-peak amplitudes smaller than 50 pA (background noise peak-to-peak amplitude is around 10 pA) were not included for the analysis, to eliminate potential contamination from nearby cells.

Values for Main Figures. Fig. 1*B*: Control, before sham exposure: 0.71 ± 0.02, after sham exposure: 0.69 ± 0.02, $n = 16$, $P = 0.55$; tinnitus, before noise exposure: 0.65 ± 0.02, after noise exposure: 0.88 ± 0.02, $n = 18$, $P < 0.001$; nontinnitus, before noise exposure: 0.69 ± 0.03, after noise exposure: 0.63 ± 0.03, $n = 17$, $P = 0.20$.

Fig. 1*C*: Control, before: 0.69 ± 0.02, after: 0.66 ± 0.04, $n = 16$, $P = 0.47$; tinnitus, before: 0.75 ± 0.03, after: 0.79 ± 0.03, $n = 18$, $P = 0.17$; nontinnitus, before: 0.73 ± 0.04, after: 0.66 ± 0.04, $n = 17$, $P = 0.14$.

Fig. 1*E*: Control, before: 0.51 ± 0.05, after: 0.53 ± 0.06, $n = 18$, $P = 0.72$; tinnitus, before: 0.60 ± 0.06, after: 0.56 ± 0.04, $n = 16$, $P = 0.61$; nontinnitus, before: 0.46 ± 0.05, after: 0.52 ± 0.04, $n = 17$, $P = 0.32$.

Fig. 1*F*: Control, before: 0.47 ± 0.04, after: 0.50 ± 0.04, $n = 18$, $P = 0.62$; tinnitus, before: 0.52 ± 0.03, after: 0.48 ± 0.03, $n = 18$, $P = 0.26$; nontinnitus, before: 0.54 ± 0.04, after: 0.52 ± 0.03, $n = 17$, $P = 0.83$.

Fig. 3*A*: Resting membrane potential, control: −62.7 ± 0.7 mV, $n = 6$, tinnitus: −62.9 ± 0.7 mV, $n = 11$, $P = 0.87$; control: −61.8 ± 1.4 mV, $n = 6$, after XE991: −62.0 ± 1.4 mV, $n = 6$, $P = 0.74$.

Fig. 3*B*: Spike threshold, control: −48.1 ± 1.0 mV, $n = 11$, tinnitus: −46.8 ± 0.5 mV, $n = 11$, $P = 0.26$; control: −48.4 ± 1.8 mV, $n = 6$; after XE991: −48.5 ± 1.7 mV, $n = 6$, $P = 0.85$.

Fig. 3*H*: 0.1 mM, 11.5% ± 3.5%, $n = 5$; 1 mM, 39.9% ± 3.7%, $n = 6$; 10 mM, 75.4% ± 6.8%, $n = 6$; 30 mM, 82.3% ± 4.3%, $n = 4$.

Fig. 4*B*: PPI startle ratio, control: 0.47 ± 0.06, $n = 16$, noise-exposed: 0.54 ± 0.03, $n = 33$, noise-exposed + retigabine: 0.47 ± 0.04, $n = 16$, noise-exposed + saline: 0.53 ± 0.06, $n = 16$, $P = 0.55$.

Fig. 4*C*: ABR threshold, control: 46.7 ± 2.7 dB, $n = 7$, noise-exposed: 51.6 ± 2.0 dB, $n = 18$, noise-exposed + retigabine: 50.2 ± 2.7 dB, $n = 7$, noise-exposed + saline: 46.7 ± 2.2 dB, $n = 7$, $P = 0.35$.

1. Turner JG, et al. (2006) Gap detection deficits in rats with tinnitus: A potential novel screening tool. *Behav Neurosci* 120(1):188–195.
2. Middleton JW, et al. (2011) Mice with behavioral evidence of tinnitus exhibit dorsal cochlear nucleus hyperactivity because of decreased GABAergic inhibition. *Proc Natl Acad Sci USA* 108(18):7601–7606.
3. Luszczki JJ (2009) Third-generation antiepileptic drugs: Mechanisms of action, pharmacokinetics and interactions. *Pharmacol Rep* 61(2):197–216.
4. Tzounopoulos T, Kim Y, Oertel D, Trussell LO (2004) Cell-specific, spike timing-dependent plasticities in the dorsal cochlear nucleus. *Nat Neurosci* 7(7):719–725.
5. Leao RM, Li S, Doiron B, Tzounopoulos T (2012) Diverse levels of an inwardly rectifying potassium conductance generate heterogeneous neuronal behavior in a population of dorsal cochlear nucleus pyramidal neurons. *J Neurophysiol* 107(11):3008–3019.

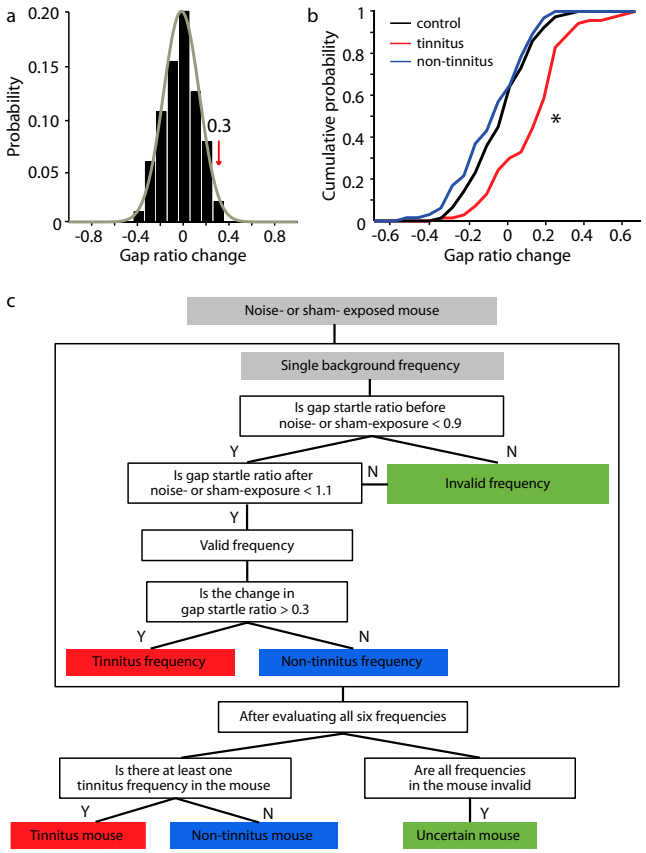

Fig. S1. Noise-induced increases in gap startle ratio for more than 0.3 is a criterion for separating tinnitus from nontinnitus mice. (*A*) Probability distribution of changes in gap startle ratio (response to gap and startle stimulus/response to startle alone) (gap ratio change) before and 1 wk after sham exposure in control mice. Changes in gap ratios represent changes in control mice between postnatal day (P)17–P20 and P24–P27 (age matched to pre- and post-noise-exposed mice). Data were fitted by a normal distribution (gray curve, $\mu = -0.01$, $\delta = 0.15$, $n = 77$). Gap ratio changes less than 0.3 (red arrow) represent 96.1% of the population in experiment and 97.8% in fitted distribution. (*B*) Cumulative probability distribution for changes in gap ratio before and after sham- or noise exposure for control (black), tinnitus (red), and nontinnitus mice (blue) (control: -0.01 ± 0.02, $n = 75$, tinnitus: 0.14 ± 0.02, $n = 70$, nontinnitus: -0.06 ± 0.02, $n = 65$, $P < 0.0001$). *$P < 0.05$. (*C*) Diagram illustrating the criteria for assessing the behavioral evidence of tinnitus. Detailed criteria in *SI Materials and Methods*.

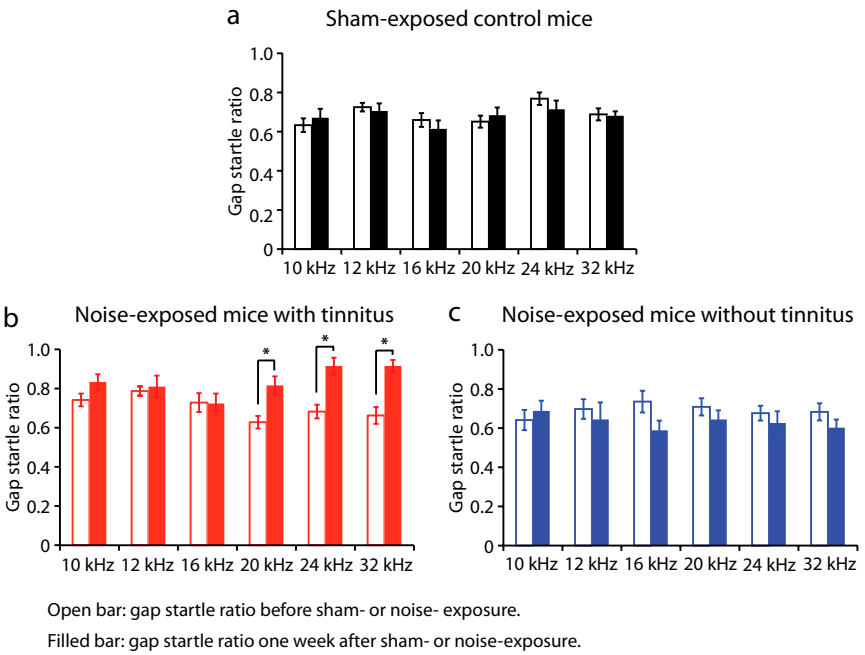

Fig. S2. Tinnitus behavior (gap detection deficit) is detected with high-frequency background sounds. Summary graph of gap startle ratio (response to gap and startle stimulus/response to startle alone) for different frequencies of background for: (*A*) control (10 kHz, before: 0.63 ± 0.03, after: 0.67 ± 0.04, $n = 13$, $P = 0.37$; 12 kHz, before: 0.73 ± 0.02, after: 0.71 ± 0.04, $n = 13$, $P = 0.64$; 16 kHz, before: 0.66 ± 0.04, after: 0.61 ± 0.04, $n = 13$, $P = 0.44$; 20 kHz, before: 0.65 ± 0.03, after: 0.68 ± 0.04, $n = 13$, $P = 0.46$; 24 kHz, before: 0.77 ± 0.03, after: 0.71 ± 0.04, $n = 12$, $P = 0.19$; 32 kHz, before: 0.69 ± 0.03, after: 0.68 ± 0.02, $n = 16$, $P = 0.87$); (*B*) tinnitus (10 kHz, before: 0.74 ± 0.03, after: 0.83 ± 0.04, $n = 13$, $P = 0.11$; 12 kHz, before: 0.79 ± 0.02, after: 0.81 ± 0.06, $n = 9$, $P = 0.67$; 16 kHz, before: 0.73 ± 0.05, after: 0.72 ± 0.05, $n = 9$, $P = 0.93$; 20 kHz, before: 0.63 ± 0.03, after: 0.82 ± 0.05, $n = 16$, $P < 0.001$; 24 kHz, before: 0.68 ± 0.03, after: 0.92 ± 0.04, $n = 12$, $P = 0.004$; 32 kHz, before: 0.66 ± 0.04, after: 0.92 ± 0.03, $n = 12$, $P < 0.0001$); and (*C*) nontinnitus mice (10 kHz, before: 0.64 ± 0.05, after: 0.69 ± 0.05, $n = 10$, $P = 0.37$; 12 kHz, before: 0.70 ± 0.05, after: 0.64 ± 0.09, $n = 7$, $P = 0.39$; 16 kHz, before: 0.74 ± 0.06, after: 0.59 ± 0.05, $n = 9$, $P = 0.06$; 20 kHz, before: 0.71 ± 0.04, after: 0.64 ± 0.05, $n = 13$, $P = 0.16$; 24 kHz, before: 0.68 ± 0.04, after: 0.63 ± 0.06, $n = 13$, $P = 0.29$; 32 kHz, before: 0.68 ± 0.04, after: 0.60 ± 0.04, $n = 15$, $P = 0.12$). *$P < 0.05$. Error bars indicate SEM.

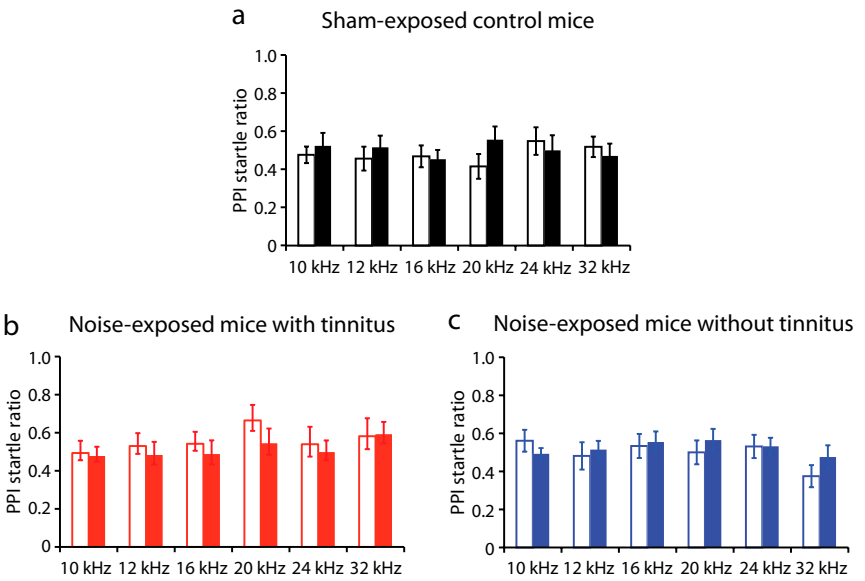

Fig. S3. PPI is not affected by noise exposure. Summary graph of PPI startle ratio (response to prepulse and startle stimulus/response to startle alone) with different frequencies of prepulse for: (*A*) control (10 kHz, before: 0.48 ± 0.04, after: 0.52 ± 0.07, $n = 15$, $P = 0.52$; 12 kHz, before: 0.46 ± 0.06, after: 0.52 ± 0.06, $n = 16$, $P = 0.52$; 16 kHz, before: 0.47 ± 0.06, after: 0.45 ± 0.05, $n = 18$, $P = 0.06$; 20 kHz, before: 0.42 ± 0.07, after: 0.56 ± 0.07, $n = 15$, $P = 0.12$; 24 kHz, before: 0.55 ± 0.07, after: 0.50 ± 0.07, $n = 16$, $P = 0.61$; 32 kHz, before: 0.52 ± 0.05, after: 0.50 ± 0.08, $n = 16$, $P = 0.61$); (*B*) tinnitus (10 kHz, before: 0.49 ± 0.05, after: 0.47 ± 0.04, $n = 17$, $P = 0.79$; 12 kHz, before: 0.53 ± 0.05, after: 0.48 ± 0.06, $n = 15$, $P = 0.49$; 16 kHz, before: 0.54 ± 0.05, after: 0.48 ± 0.07, $n = 14$, $P = 0.51$; 20 kHz, before: 0.66 ± 0.07, after: 0.54 ± 0.07, $n = 12$, $P = 0.28$; 24 kHz, before: 0.54 ± 0.08, after: 0.49 ± 0.05, $n = 11$, $P = 0.64$; 32 kHz, before: 0.58 ± 0.09, after: 0.59 ± 0.06, $n = 14$, $P = 0.69$) and; (*C*) nontinnitus mice (10 kHz, before: 0.56 ± 0.06, after: 0.49 ± 0.03, $n = 16$, $P = 0.31$; 12 kHz, before: 0.48 ± 0.07, after: 0.51 ± 0.05, $n = 14$, $P = 0.75$; 16 kHz, before: 0.53 ± 0.06, after: 0.55 ± 0.06, $n = 15$, $P = 0.84$; 20 kHz, before: 0.50 ± 0.06, after: 0.55 ± 0.06, $n = 15$, $P = 0.50$; 24 kHz, before: 0.53 ± 0.06, after: 0.53 ± 0.04, $n = 15$, $P = 0.99$; 32 kHz, before: 0.37 ± 0.06, after: 0.48 ± 0.06, $n = 17$, $P = 0.13$). Error bars indicate SEM.

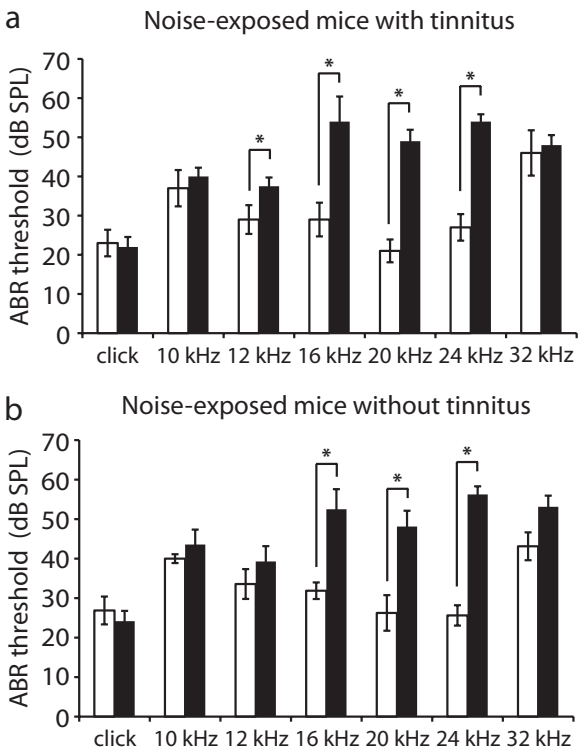

Fig. S4. ABR thresholds are equally elevated one week after noise exposure in both tinnitus and nontinnitus mice. Summary graph showing ABR thresholds before (opens bars) and 1 wk after noise exposure (filled bars) in: (*A*) tinnitus (click, before: 23.0 ± 3.4 dB, after: 22.0 ± 2.5 dB, $n = 5$, $P = 0.28$; 10 kHz, before: 37.0 ± 4.6 dB, after: 40.0 ± 2.2 dB, $n = 5$, $P = 0.41$; 12 kHz, before: 29.0 ± 3.7 dB, after: 37.5 ± 2.2 dB, $n = 5$, $P = 0.04$; 16 kHz, before: 29.0 ± 4.3 dB, after: 54.0 ± 6.4 dB, $n = 5$, $P = 0.01$; 20 kHz, before: 21.0 ± 2.9 dB, after: 49.0 ± 2.9 dB, $n = 5$, $P < 0.001$; 24 kHz, before: 27.0 ± 3.4 dB, after: 54.0 ± 1.9 dB, $n = 5$, $P < 0.001$; 32 kHz, before: 46.0 ± 5.8 dB, after: 48.0 ± 2.5 dB, $n = 5$, $P = 0.73$); and (*B*) nontinnitus mice (click, before: 26.9 ± 3.5 dB, after: 24.2 ± 2.6 dB, $n = 7$, $P = 0.2$; 10 kHz, before: 40.0 ± 1.1 dB, after: 43.6 ± 3.8 dB, $n = 7$, $P = 1.00$; 12 kHz, before: 33.6 ± 3.8 dB, after: 39.9 ± 3.9 dB, $n = 7$, $P = 0.22$; 16 kHz, before: 31.8 ± 2.1 dB, after 52.5 ± 5.1 dB, $n = 7$, $P = 0.04$; 20 kHz, before: 26.3 ± 4.5 dB, after: 48.1 ± 4.0 dB, $n = 7$, $P = 0.005$; 24 kHz, before: 25.6 ± 2.6 dB, after: 56.3 ± 2.1 dB, $n = 7$, $P < 0.001$; 32 kHz, before: 43.1 ± 3.5 dB, after: 53.1 ± 2.8 dB, $n = 18$, $P = 0.07$). *$P < 0.05$. Error bars indicate SEM.

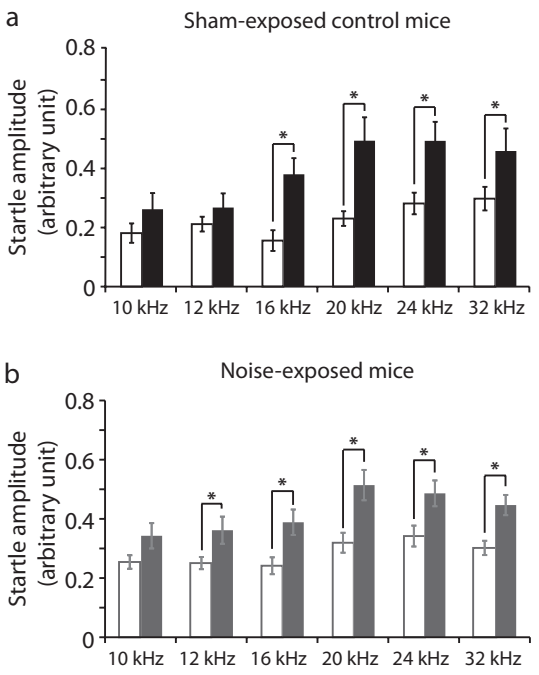

Fig. S5. Acoustic startle amplitude is increased in mice between P17–P20 and P24–P27 in an age-dependent manner, but the increase is unaffected by noise exposure. Acoustic startle amplitude before and 1 wk after sham- or noise exposure for: (*A*) control (10 kHz, before: 0.18 ± 0.03, after: 0.26 ± 0.05, $n = 11$, $P = 0.21$; 12 kHz, before: 0.21 ± 0.03, after: 0.27 ± 0.05, $n = 11$, $P = 0.26$; 16 kHz, before: 0.15 ± 0.04, after: 0.38 ± 0.05, $n = 11$, $P = 0.01$; 20 kHz, before: 0.23 ± 0.02, after: 0.49 ± 0.08, $n = 11$, $P = 0.007$; 24 kHz, before: 0.28 ± 0.04, after: 0.49 ± 0.06, $n = 11$, $P = 0.01$; 32 kHz, before: 0.30 ± 0.03, after: 0.46 ± 0.08, $n = 11$, $P = 0.03$); and (*B*) noise-exposed mice (10 kHz, before: 0.25 ± 0.02, after: 0.34 ± 0.04, $n = 17$, $P = 0.06$; 12 kHz, before: 0.25 ± 0.02, after: 0.36 ± 0.05, $n = 17$, $P = 0.04$; 16 kHz, before: 0.24 ± 0.03, after: 0.38 ± 0.04, $n = 17$, $P = 0.006$; 20 kHz, before: 0.32 ± 0.03, after: 0.51 ± 0.05, $n = 17$, $P = 0.004$; 24 kHz, before: 0.34 ± 0.04, after: 0.48 ± 0.04, $n = 17$, $P = 0.005$; 32 kHz, before: 0.30 ± 0.02, after: 0.45 ± 0.03, $n = 17$, $P = 0.001$). *$P < 0.05$. Error bars indicate SEM.

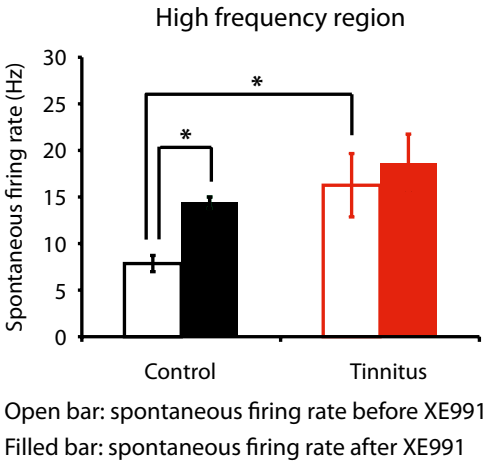

Fig. S6. XE991 equalizes the spontaneous firing rate between control and tinnitus mice. Summary graph of spontaneous firing rate of fusiform cells recorded from high-frequency DCN regions in control (black) and in tinnitus mice (red), before and after XE991 application (before XE991: control, 7.9 ± 0.9 Hz, $n = 6$, tinnitus, 16.3 ± 3.4 Hz, $n = 7$, $P = 0.049$; after XE991: control, 14.3 ± 0.6 Hz, $n = 6$, $P < 0.001$ compared with control before XE991; after XE991: tinnitus, 18.6 ± 3.1 Hz, $n = 7$, $P = 0.232$ compared with control after XE991). *$P < 0.05$. Error bars indicate SEM.

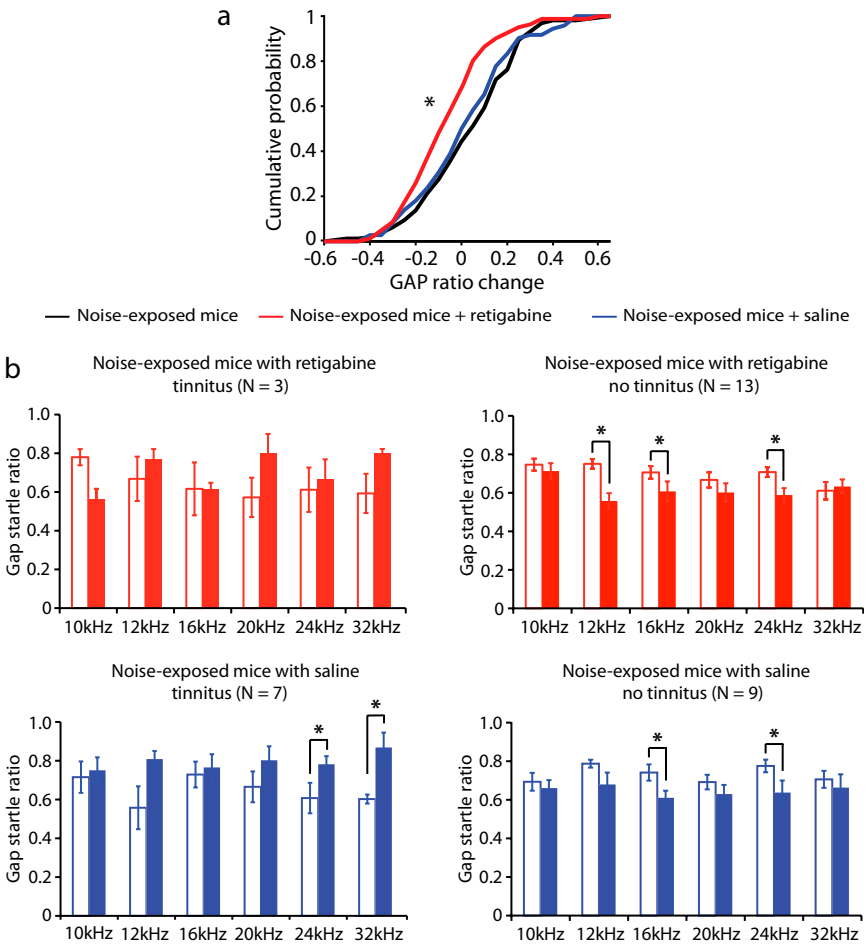

Fig. S7. Retigabine administration prevents the development of tinnitus. (*A*) Cumulative probability distribution for changes in gap startle ratio before and 1 wk after noise exposure (gap ratio change) for noise-exposed only mice (black), noise-exposed mice with retigabine injection (red), and noise-exposed mice with saline injection (blue) (noise-exposed: 0.04 ± 0.02, $n = 135$, noise-exposed + retigabine: −0.05 ± 0.02, $n = 81$, noise-exposed + saline: 0.03 ± 0.03, $n = 72$, $P = 0.002$). (*B*) Summary graph of gap startle ratio (response to gap and startle stimulus/response to startle alone) for different frequencies of background for: noise-exposed mice treated with retigabine that showed tinnitus (*Upper Left*, 10 kHz, before: 0.78 ± 0.04, after: 0.56 ± 0.05, $n = 3$; 12 kHz, before: 0.67 ± 0.11, after: 0.77 ± 0.06, $n = 2$; 16 kHz, before: 0.62 ± 0.14, after: 0.61 ± 0.04, $n = 3$, 20 kHz, before: 0.57 ± 0.10, after: 0.80 ± 0.10, $n = 3$; 24 kHz, before: 0.61 ± 0.11, after: 0.66 ± 0.11, $n = 3$; 32 kHz, before: 0.59 ± 0.10, after: 0.80 ± 0.02, $n = 3$), noise-exposed mice treated with retigabine that did not show tinnitus (*Upper Right*, 10 kHz, before: 0.75 ± 0.03, after: 0.71 ± 0.04, $n = 13$, $P = 0.37$; 12 kHz, before: 0.75 ± 0.03, after: 0.56 ± 0.04, $n = 9$, $P < 0.001$; 16 kHz, before: 0.71 ± 0.03, after: 0.61 ± 0.05, $n = 11$, $P = 0.03$; 20 kHz, before: 0.67 ± 0.04, after: 0.60 ± 0.05, $n = 10$, $P = 0.21$; 24 kHz, before: 0.71 ± 0.03, after: 0.59 ± 0.04, $n = 11$, $P = 0.02$; 32 kHz, before: 0.61 ± 0.05, after: 0.63 ± 0.04, $n = 11$, $P = 0.71$), noise-exposed mice treated with saline that showed tinnitus (*Lower Left*, 10 kHz, before: 0.72 ± 0.08, after: 0.75 ± 0.07, $n = 6$, $P = 0.76$; 12 kHz, before: 0.56 ± 0.11, after: 0.81 ± 0.04, $n = 4$, $P = 0.08$; 16 kHz, before: 0.73 ± 0.07, after: 0.77 ± 0.09, $n = 6$, $P = 0.55$; 20 kHz, before: 0.67 ± 0.08, after: 0.80 ± 0.07, $n = 7$, $P = 0.13$; 24 kHz, before: 0.61 ± 0.08, after: 0.78 ± 0.04, $n = 6$, $P = 0.04$; 32 kHz, before: 0.60 ± 0.02, after: 0.87 ± 0.8, $n = 6$, $P = 0.02$) and noise-exposed mice treated with saline that did not show tinnitus (*Lower Right*, 10 kHz, before: 0.69 ± 0.05, after: 0.66 ± 0.04, $n = 11$, $P = 0.52$; 12 kHz, before: 0.79 ± 0.02, after: 0.68 ± 0.06, $n = 8$, $P = 0.14$; 16 kHz, before: 0.74 ± 0.04, after: 0.61 ± 0.04, $n = 11$, $P = 0.01$; 20 kHz, before: 0.69 ± 0.04, after: 0.63 ± 0.05, $n = 11$, $P = 0.18$; 24 kHz, before: 0.78 ± 0.03, after: 0.64 ± 0.06, $n = 11$, $P = 0.02$; 32 kHz, before: 0.71 ± 0.04, after: 0.66 ± 0.07, $n = 10$, $P = 0.49$). *$P < 0.05$. Error bars indicate SEM.

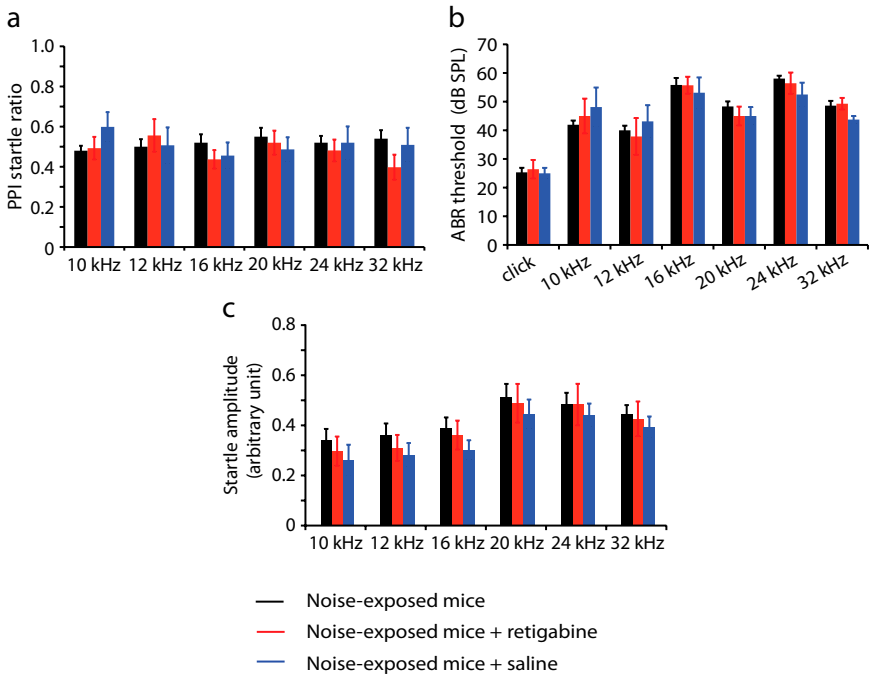

Fig. S8. Retigabine administration does not affect PPI; auditory brainstem response (ABR) thresholds; startle reflex amplitude. (*A*) Summary graph of PPI startle ratio (response to prepulse and startle stimulus/response to startle alone) for different frequencies of prepulse 1 wk after noise exposure in noise-exposed only mice (black), noise-exposed mice with retigabine injection (red), and noise-exposed mice with saline injection (blue) (10 kHz, noise-exposed: 0.48 ± 0.02, $n = 33$, noise-exposed + retigabine: 0.49 ± 0.06, $n = 15$, noise-exposed + saline: 0.60 ± 0.07, $n = 13$, $P = 0.13$; 12 kHz, noise-exposed: 0.50 ± 0.04, $n = 29$, noise-exposed + retigabine: 0.56 ± 0.08, $n = 14$, noise-exposed + saline: 0.51 ± 0.09, $n = 11$, $P = 0.77$; 16 kHz, noise-exposed: 0.52 ± 0.04, $n = 29$, noise-exposed + retigabine: 0.44 ± 0.05, $n = 15$, noise-exposed + saline: 0.46 ± 0.07, $n = 16$, $P = 0.49$; 20 kHz, noise-exposed: 0.55 ± 0.04, $n = 27$, noise-exposed + retigabine: 0.52 ± 0.06, $n = 14$, noise-exposed + saline: 0.49 ± 0.06, $n = 12$, $P = 0.70$; 24 kHz, noise-exposed: 0.52 ± 0.03, $n = 26$, noise-exposed + retigabine: 0.48 ± 0.05, $n = 14$, noise-exposed + saline: 0.52 ± 0.08, $n = 13$, $P = 0.82$; 32 kHz, noise-exposed: 0.54 ± 0.04, $n = 30$, noise-exposed + retigabine: 0.40 ± 0.06, $n = 16$, noise-exposed + saline: 0.51 ± 0.09, $n = 14$, $P = 0.21$). (*B*) Summary graph showing ABR thresholds 1 wk after noise exposure for noise-exposed only mice, noise-exposed mice with retigabine injection and noise-exposed mice with saline injection (click, noise-exposed: 25.3 ± 1.6 dB, $n = 15$, noise-exposed + retigabine: 26.4 ± 3.2 dB, $n = 7$, noise-exposed + saline: 25.0 ± 1.9 dB, $n = 7$, $P = 0.9$; 10 kHz, noise-exposed: 41.9 ± 1.5 dB, $n = 18$, noise-exposed + retigabine: 45.0 ± 6.1 dB, $n = 7$, noise-exposed + saline: 48.1 ± 6.8 dB, $n = 7$, $P = 0.5$; 12 kHz, noise-exposed: 40.0 ± 1.6 dB, $n = 18$, noise-exposed + retigabine: 37.9 ± 6.4 dB, $n = 7$, noise-exposed + saline: 43.1 ± 5.7 dB, $n = 7$, $P = 0.69$; 16 kHz, noise-exposed: 55.8 ± 2.4 dB, $n = 18$, noise-exposed + retigabine: 55.7 ± 3.0 dB, $n = 7$, noise-exposed + saline: 53.1 ± 5.3 dB, $n = 7$, $P = 0.86$; 20 kHz, noise-exposed: 48.3 ± 1.8 dB, $n = 18$, noise-exposed + retigabine: 45.0 ± 3.3 dB, $n = 7$, noise-exposed + saline: 45.0 ± 3.2 dB, $n = 7$, $P = 0.50$; 24 kHz, noise-exposed: 58.1 ± 1.0 dB, $n = 18$, noise-exposed + retigabine: 56.4 ± 3.7 dB, $n = 7$, noise-exposed + saline: 52.5 ± 4.11 dB, $n = 7$, $P = 0.26$; 32 kHz, noise-exposed: 48.6 ± 1.65 dB, $n = 18$; noise-exposed + retigabine: 49.3 ± 2.0 dB, $n = 16$, noise-exposed + saline: 43.7 ± 1.3 dB, $n = 7$, $P = 0.17$). (*C*) Summary graph showing acoustic startle amplitude 1 wk after noise exposure for noise-exposed only mice, noise-exposed mice with retigabine injection and noise-exposed mice with saline injection (noise-exposed: 0.34 ± 0.04, $n = 17$, noise-exposed + retigabine: 0.30 ± 0.06, $n = 14$, noise-exposed + saline: 0.26 ± 0.06, $n = 14$, $P = 0.57$; 12 kHz, noise-exposed: 0.36 ± 0.05, $n = 17$, noise-exposed +retigabine: 0.31 ± 0.05, $n = 14$, noise-exposed + saline: 0.30 ± 0.04, $n = 14$, $P = 0.53$; 16 kHz, noise-exposed: 0.39 ± 0.04, $n = 17$, noise-exposed + retigabine: 0.36 ± 0.06, $n = 14$, noise-exposed + saline: 0.30 ± 0.04, $n = 14$, $P = 0.39$; 20 kHz, noise-exposed: 0.51 ± 0.05, $n = 17$, noise-exposed + retigabine: 0.49 ± 0.08, $n = 14$, noise-exposed + saline: 0.45 ± 0.06, $n = 14$, $P = 0.75$; 24 kHz, noise-exposed: 0.49 ± 0.04, $n = 18$, noise-exposed + retigabine: 0.48 ± 0.08, $n = 14$, saline: 0.44 ± 0.05, $n = 14$, $P = 0.81$; 32 kHz, noise-exposed: 0.45 ± 0.03, $n = 17$, noise-exposed + retigabine: 0.43 ± 0.07, $n = 14$, noise-exposed + saline: 0.40 ± 0.04, $n = 14$, $P = 0.7$). Error bars indicate SEM.

Table S1. Intrinsic properties of fusiform cells from high-frequency region of DCN in control and tinnitus mice

Mice	Input resistance (MΩ)	Spike amplitude (mV)	Depolarization slope (V/s)	Hyperpolarization slope (V/s)	Half height width (ms)	fAHP (mV)
Control	63.61 ± 4.28	38.92 ± 1.29	161.05 ± 5.80	−156.06 ± 5.45	0.30 ± 0.01	22.36 ± 1.37
Tinnitus	67.55 ± 2.40	38.28 ± 1.02	147.32 ± 4.59	−136.75 ± 4.88	0.34 ± 0.02	22.11 ± 1.08

All recordings were performed in fusiform cells in the high-frequency region of the DCN (input resistance, control: $n = 8$, tinnitus: $n = 12$, $P = 0.62$; spike amplitude, control: $n = 11$, tinnitus: $n = 11$, $P = 0.67$; depolarization slope, control: $n = 11$, tinnitus: $n = 11$, $P = 0.07$; hyperpolarization slope, control: $n = 11$, tinnitus, $n = 11$, $P = 0.07$; half height width, control: $n = 11$, tinnitus: $n = 11$, $P = 0.67$; fAHP, control: $n = 11$, tinnitus: $n = 11$, $P = 0.88$). Depolarization slope: maximum depolarizing slope; hyperpolarization slope: minimum hyperpolarizing slope; fAHP: fast afterhyperpolarization.